Initiation and re-initiation of DNA unwinding by the *Escherichia coli* Rep helicase

Taekjip Ha*, Ivan Rasnik*, Wei Cheng†, Hazen P. Babcock‡ George H. Gauss†, Timothy M. Lohman† & Steven Chu‡

* *Department of Physics, University of Illinois, Urbana, Illinois 61801, USA*
† *Department of Biochemistry and Molecular Biophysics, Washington University School of Medicine, St Louis, Missouri 63110, USA*
‡ *Department of Physics, Stanford University, Stanford, California 94305, USA*

Helicases are motor proteins that couple conformational changes induced by ATP binding and hydrolysis with unwinding of duplex nucleic acid[1–3], and are involved in several human diseases. Some function as hexameric rings[4], but the functional form of non-hexameric helicases has been debated[5–10]. Here we use a combination of a surface immobilization scheme and single-molecule fluorescence assays—which do not interfere with biological activity—to probe DNA unwinding by the *Escherichia coli* Rep helicase. Our studies indicate that a Rep monomer uses ATP hydrolysis to move toward the junction between single-stranded and double-stranded DNA but then displays conformational fluctuations that do not lead to DNA unwinding. DNA unwinding initiates only if a functional helicase is formed via additional protein binding. Partial dissociation of the functional complex during unwinding results in interruptions ('stalls') that lead either to duplex rewinding upon complete dissociation of the complex, or to re-initiation of unwinding upon re-formation of the functional helicase. These results suggest that the low unwinding processivity observed *in vitro* for Rep is due to the relative instability of the functional complex. We expect that these techniques will be useful for dynamic studies of other helicases and protein–DNA interactions.

Two single-molecule approaches have been used to visualize DNA unwinding by the highly processive *E. coli* RecBCD helicase/nuclease[11,12] with resolutions up to 100 base pairs (bp)[12]. However, many helicases display only limited processivity *in vitro*, so methods with higher base-pair resolution are desired. We have used the single-molecule fluorescence resonance energy transfer (FRET) technique[13–16] to measure structural changes of DNA upon the action of *E. coli* Rep helicase. Not only could we detect DNA unwinding with ≤10-bp resolution, but we also were able to observe events that are difficult to examine in bulk solution, such as stalls, rewinding of the DNA duplex and re-initiation of unwinding by a stalled enzyme–DNA complex.

To probe the initiation of DNA unwinding with maximum sensitivity we used an 18-bp or 40-bp duplex with a 3′-$(dT)_{20}$ tail with a donor (Cy3) and an acceptor (Cy5) fluorophore attached to the junction between single-stranded DNA (ssDNA) and double-stranded DNA (dsDNA) (DNA I and II, Fig. 1i). DNA molecules were specifically immobilized to a polymer-coated surface[17], and were imaged using an evanescent field microscope[15]. We then rapidly (<0.2 s) delivered a solution containing both Rep and ATP, and recorded the time records of unwinding via FRET (Fig. 1i). Before unwinding begins, the distance, R, between the two dyes is small ($E_{FRET} \approx 1$; $E_{FRET} \equiv 1/[1 + I_D/I_A]$ is an approximation for FRET efficiency, $1/([1 + (R/R_0)^6]$, where I_D and I_A are intensities for donor and acceptor respectively and $R_0 \approx 6$ nm). As the DNA is unwound, the time-averaged R increases (E_{FRET} decreases). If the DNA is fully unwound, the donor strand diffuses away from the surface and the fluorescence signal abruptly disappears, clearly marking the completion of unwinding. In contrast, dissociation of the helicase during unwinding can lead to rapid DNA rewinding ($E_{FRET} \rightarrow \sim 1$). The elimination of only one component among ATP, Rep and Mg^{2+} or the replacement of ATP by its poorly hydrolysed analogues (adenosine 5′-[γ-thio]triphosphate or adenosine 5′-(β,γ-imido)triphosphate) abolished all unwinding signals.

After adding Rep protein, which is a monomer in the absence of DNA[18], and ATP, a characteristic time elapsed before unwinding was initiated. Its average, τ_{UI}, is inversely proportional to [Rep] (above 20 nM) and the rate of unwinding initiation thus determined is $1.2 \times 10^5\ M^{-1}\ s^{-1}$ (Fig. 1j), close to the value of $(1.5 \pm 0.1) \times 10^5\ M^{-1}\ s^{-1}$ measured in bulk solution[10]. Once initiated, unwinding of the 18-bp duplex proceeds quickly to completion (Fig. 1a, b). The duration of the unwinding events, an average of 0.4 ± 0.2 s, is also consistent with bulk-solution values determined using DNA with and without dye labels[10,19]. Therefore, neither DNA immobilization nor dye attachment significantly affects DNA unwinding. The characteristics of 18-bp unwinding are independent of [Rep], hence unwinding probably results from the action of a well-defined entity. Several intermediate E_{FRET} values, indicative of partially unwound intermediates, could be resolved during unwinding. Complete unwinding of a 40-bp duplex takes longer, about 1 s if uninterrupted (Fig. 1c, d); however, stalls (defined as interruptions in the E_{FRET} decrease which persist for longer than 1 s) are observed in ~70% of the 40-bp unwinding events (see Fig. 1e–h, and discussion below). Before signal termination, the E_{FRET} for the 40-bp duplex drops to lower values than for the 18-bp duplex, probably because the time-averaged R reaches larger values before complete unwinding.

In order to correlate the unwinding data with the DNA-binding properties of Rep, we designed DNA III (Fig. 2), which should be sensitive to changes in the time-averaged conformation of the

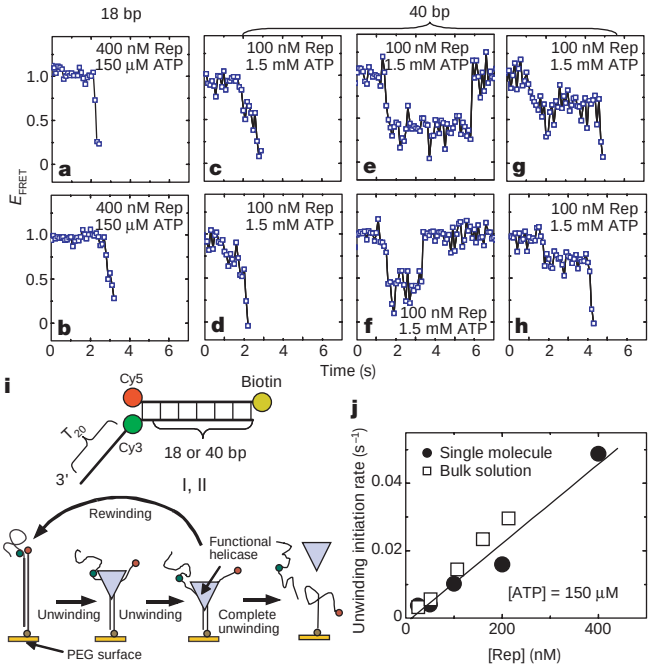

Figure 1 FRET assay for single DNA unwinding. **a**–**h**, Single DNA unwinding time records (100-ms bins) typical of four distinct patterns: complete unwinding of 18 bp (**a**, **b**), complete unwinding (**c**, **d**), stall and DNA rewinding (**e**, **f**), and stall and unwinding re-initiation (**g**, **h**) of 40 bp. When unwinding is completed (**a**–**d**, **g**–**h**), the donor strand quickly diffuses away, abruptly terminating the signal. **i**, The experimental scheme (see text). **j**, The rate of unwinding initiation (the inverse of time between the delivery of enzyme with ATP and the unwinding initiation, averaged over >50 events for each [Rep]) versus [Rep]. A linear fit and bulk-solution values[10] are shown.

ssDNA tail induced upon Rep binding. In the absence of ATP, we observed two binding conformations of the Rep monomer/DNA complex, with little specificity for the ss/dsDNA junction (Supplementary Information Figs I and II).

In the presence of ATP, if [Rep] < 2 nM, DNA unwinding rarely occurs (experiments with DNA I did not detect any unwinding). Hence, under these conditions, we can probe the conformations of DNA III induced by Rep binding. Individual time traces showed brief bursts of fluctuations (Fig. 2a and Supplementary Information Fig. III) that we interpret as reflecting Rep monomer binding, conformational fluctuations, and dissociation. Our interpretation is based on the following observations. (1) The average burst duration ($\sim$4 s) is independent of [Rep], and matches the monomer dissociation rate ($\sim 0.24\,s^{-1}$) measured in bulk solution[10]. (2) The number of bursts per second is linearly dependent on [Rep] with a slope of $0.7\times10^{7}\,M^{-1}\,s^{-1}$ (Supplementary Information Fig. III), slightly lower than the bulk solution rate constant ($\sim 2\times10^{7}\,M^{-1}\,s^{-1}$)[10] for monomer binding to ssDNA (dT_{16}). This difference is understandable, as intermediate steps appear necessary between the Rep monomer binding and the observation of the burst (see below), and the steps involved in ssDNA translocation may not occur with unit probability. (3) The reciprocal experiment where biotinylated Rep (Rep-BCCP) monomers were immobilized with DNA III (without biotin) and ATP in solution showed similar fluctuations ($\sim$3 s average duration; Fig. 2b) when DNA binds to the Rep-BCCP monomer, indicating that the fluctuations are not caused by interactions of multiple monomers. In a separate experiment using DNA I (without biotin) and immobilized Rep-BCCP, no unwinding was observed, whereas the DNA binds transiently to the protein for the same average duration.

ATP hydrolysis appears necessary to observe these bursts, as they were not observed when ATPγS (with almost identical binding kinetics to ATP, but 500 × lower hydrolysis rate; ref. 20) were used. No such fluctuations were observed with AMPPNP, or with an ATPase deficient mutant RepK28I in the presence of ATP[21]. They appear specific for a 3′-ss/dsDNA junction because a DNA molecule possessing the same 18-bp duplex but with a 5′-$(dT)_{19}$ tail did not show such bursts. Combined with the evidence that PcrA, a structural homologue of Rep, can translocate as a monomer along ssDNA with a 3′ to 5′ directional bias at a rate of $\sim$50 bases s^{-1} (refs 9, 22), and our bulk-solution observation that Rep monomers appear able to move with the same directionality at a faster rate (C. Fischer, J. Hsieh and T.M.L., unpublished results), we interpret the fluctuations as the end result of Rep monomer's translocation toward the junction. Further evidence that a burst occurs after translocation (as opposed to reflecting translocation itself, which would be too fast to be observed here) is obtained from data on the effect of [ATP] and tail length (Supplementary Information Fig. III).

These fluctuations appear futile—that is, they do not lead to DNA unwinding, as experiments with DNA I under the same conditions did not detect unwinding. Therefore, DNA unwinding is not a simple consequence of a Rep monomer's ability to translocate along ssDNA toward the junction, where it might trap ssDNA formed transiently at the junction via thermal fraying of the duplex. Instead, there is a slow, rate-limiting step required for initiating DNA unwinding after monomer positioning near the junction.

We considered two possibilities for this rate-limiting step. The first is that the Rep monomer must undergo slow conformational transition(s) to a functional monomeric helicase. In this case, once binding near the junction is saturated, the unwinding initiation rate should remain constant even at increased [Rep]. The second possibility involves additional protein binding. Then, the unwinding initiation rate would depend on [Rep] even after the junction is saturated; a linear dependence would be expected if two monomers are required, and so on. Saturation of the ss/dsDNA junction by a monomer indeed occurs at [Rep] $\geq$ 20 nM (DNA III showed continuous fluctuations similar to the fluctuations within a burst shown in Fig. 2a, probably because a new monomer occupies the junction as soon as the junction becomes unoccupied by the previous one; Supplementary Information Fig. IV). But the unwinding initiation rate continues to increase linearly with [Rep] up to 400 nM (Fig. 1j), favouring the second model. Therefore, the rate-limiting step for DNA unwinding initiation involves the interaction of more than one Rep monomer (our data are consistent with two, but future experiments, using for example dye-labelled proteins, will directly address this question), independently confirming conclusions based on pre-steady-state single-turnover kinetic studies performed in bulk solution[10].

Our single-molecule study further indicates that the Rep monomer indeed uses ATP hydrolysis to position itself near the ss/dsDNA junction, in agreement with the main evidence suggesting that a PcrA monomer has helicase activity[5,9,22], yet DNA unwinding is not initiated until the interaction with additional protein(s) activates the unwinding. The present work also provides a more sensitive test for monomer activity because partial unwinding of a small fraction of DNA molecules (<3%) would be very difficult to detect in a bulk-solution stopped-flow study, whereas even transient unwinding would be detectable from single molecules. In addition, the DNA does not need to be incubated with proteins in the absence of ATP, which is necessary for measuring the early phase of unwinding in bulk solution. We can therefore rule out concerns that a Rep monomer/DNA complex may exist in an inactive form that cannot be rescued by adding ATP afterwards.

The single-molecule studies reported here offer insight into why Rep and many other helicases display only limited unwinding processivities *in vitro*. We observed frequent stalls of the Rep helicase during the course of unwinding a 40-bp duplex (DNA II in Fig. 1). Over two-thirds of the DNA-unwinding events resulted in stalls (Fig. 1e–h) which, in most cases, led to complete DNA rewinding (Fig. 1e, f). The average stall duration was $\sim$4 s, longer than the time it takes to unwind the duplex without a stall ($\sim$1 s, Fig. 1c, d), but

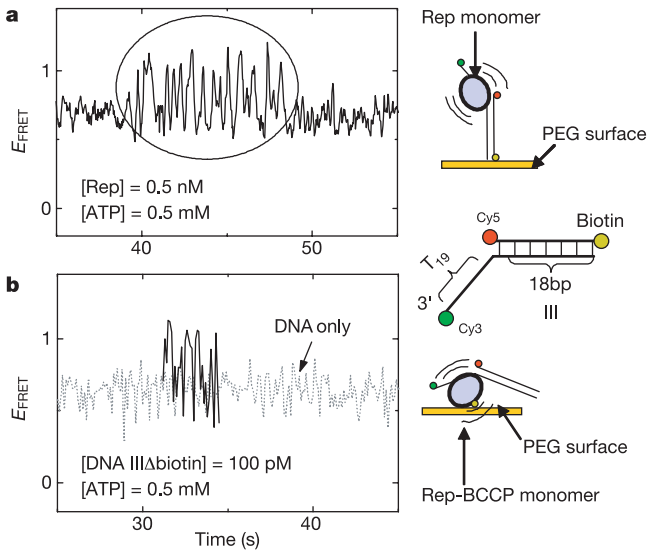

Figure 2 ATP-dependent, junction-specific fluctuations of Rep monomer. **a**, A burst of E_{FRET} fluctuations (circled) is caused by enzyme binding to surface-immobilized DNA III and conformational fluctuations (33-ms bins). **b**, A burst is observed when DNA III (minus biotin) molecules bind to a surface-immobilized, biotinylated Rep (Rep-BCCP) monomer. Fluorescence signal is detectable only during the burst (100-ms bins). Also shown is a typical trace obtained from immobilized DNA III only (grey) for comparison. Accompanying cartoons illustrate Rep monomer conformational fluctuations with either DNA or protein immobilized.

close to the dissociation timescale of a Rep monomer bound at a ss/dsDNA junction (~4 s) measured via ATP-dependent, junction-specific fluctuations (Fig. 2a). This suggests that the stalls occur as a result of partial dissociation of a functional helicase, and that the DNA re-anneals only when the remaining bound monomer, which is unable to continue unwinding, dissociates.

This interpretation is further supported by the observation that a fraction of the stalled complexes can re-initiate unwinding, resulting in completion of unwinding (Fig. 1g, h). Re-initiation was not observed in the absence of free Rep protein (that is, Rep in solution, but not associated with any DNA), and the fraction of stalled complexes that re-initiate unwinding increases with increasing concentration of free Rep (Fig. 3a). Hence, the interaction with additional Rep protein(s) appears to be responsible for the restart of stalled complexes. The fraction of stalled complexes that re-initiate unwinding also increases with increasing [ATP] (Fig. 3b). Therefore, an ATP-hydrolysis-driven process, potentially ssDNA translocation of another monomer towards the stall site, may promote functional helicase reassembly.

Overall, our analysis suggests that the limited processivity observed for Rep helicase *in vitro* is due to the relative instability of the functional helicase complex during unwinding. Such instability may contribute to the low unwinding processivities observed for many other helicases *in vitro*. *In vivo*, the relative instability of the helicase complex may enable the regulation of the unwinding activity via other factors that stabilize the complex. For Rep, ϕX174 gene A protein *in vivo* enables Rep to unwind at least 7,000 bp processively[23]. Our observation of stalled monomers also rules out the possibility that a Rep monomer can unwind DNA processively once a functional multi-Rep complex has initiated unwinding.

The cartoon in Fig. 3c summarizes our current view. After binding to a 3′ ssDNA tail, a Rep monomer hydrolyses ATP to translocate (3′ to 5′) towards the ss-dsDNA junction. The monomer displays futile conformational fluctuations either until it dissociates or until additional monomer(s) binds to form a functional helicase that can then initiate unwinding. Unwinding stalls occur if the functional helicase partially dissociates, leaving a monomer at the junction that cannot unwind, thus preventing DNA rewinding; unwinding can resume only if a functional helicase reassembles at the stall site. Future experiments using fluorescently labelled proteins may be able to observe the coupling between the protein conformational changes and unwinding activity by simultaneously measuring them on single DNA molecules. □

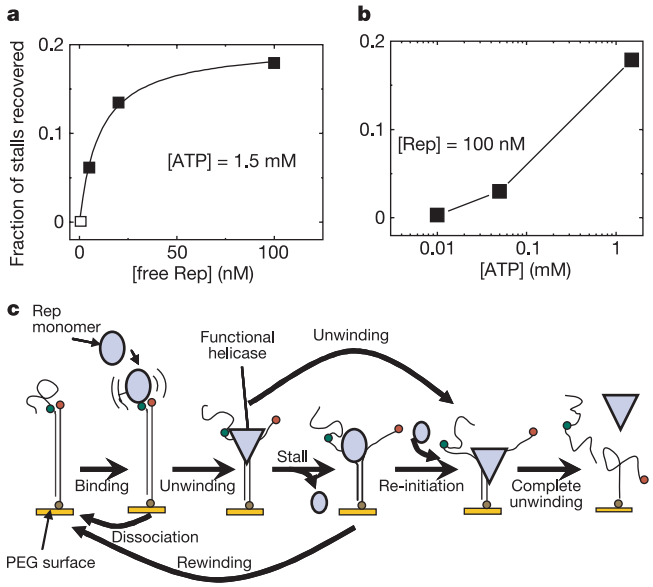

Figure 3 Mechanism of unwinding stall and re-initiation. **a**, Fraction of stalls recovered versus the concentration of free Rep (filled squares). The open square represents the observation that no stall recovery occurred if the unwinding is initiated by adding ATP and trap DNA (5 μM dT_{16}) onto immobilized DNA II incubated with 200 nM Rep. A fit to the data according to $(A[\text{Rep}])/(B + [\text{Rep}])$ is also shown ($A = 0.2$, $B = 10.4$ nM). Its saturation may imply the presence of other necessary steps or conformational changes that compete with dissociation. **b**, Fraction of stalls recovered versus [ATP]. At least 100 stalls were analysed for each condition in **a** and **b**. **c**, Unwinding mechanism.

Methods

DNA preparation

5′-Cy5-GCCTCGCTGCCGTCGCCA-3′ biotin and 5′-TGGCGACGGCAGCGAGGC-Cy3-$(T)_{20}$-3′ for DNA I, 5′-Cy5-GCCCTGCTGCCGACCAACGATGGTTACATTCCC GCTGCTG-3′ biotin and 5′-CAGCAGCGGGAATGTAACCATCGTTGGTCGGCAG CAGGGC-Cy3-$(T)_{20}$-3′ for DNA II. For DNA III, the second strand of DNA I is replaced by 5′-TGGCGACGGCAGCGAGGC-$(T)_{19}$-Cy3-T-3′. Cy3 and Cy5 were incorporated in phosphoramidite forms, and biotin was added as BiotinTEG CPG (all three from Glen Research) during oligonucleotide synthesis. DNA was gel purified and annealed in a buffer containing 10 mM Tris , 0.5 M NaCl , pH 8.0.

Protein preparation

Wild-type Rep and Rep-BCCP were purified as described[24]. Construction of Rep-BCCP is described in Supplementary Information Fig. II legend. The Stopped-flow fluorescence unwinding signal[19] for Rep-BCCP reaches saturation at [Rep-BCCP] = 200 nM and showed an unwinding stepping rate, assuming 4-bp step size, of 11.5 ± 0.5 s^{-1}, in agreement with 14.3 ± 1.1 s^{-1} for wild-type Rep[10].

Single-molecule measurements

Quartz slides were treated with an amino-silane reagent, Vectabond (Vector), and then incubated with polyethylene glycol (PEG, Shearwater Polymers, containing 20% methoxy-PEG-succinimidyl succinate and 0.25% biotin-PEG-OCH_2CH_2-CO_2-NHS) in 0.1 M sodium bicarbonate (pH 8.3) for 3 h. Streptavidin solution (0.2 mg ml^{-1}) was applied and washed away before addition of biotinylated DNA solution (10–50 pM, Tris 10 mM, NaCl 50 mM, pH 8). Adsorption of Rep protein was reduced by >1,000 × on this surface, compared to bovine serum albumin (BSA)-coated or bare glass, and solution Rep activities were faithfully reproduced. Rep-BCCP was immobilized similarly (details in Supplementary Information Fig. II). Single-molecule measurements were done at room temperature in a buffer containing 20 mM Tris (pH 7.5), 6 mM NaCl, 1.7 mM $MgCl_2$, 10% glycerol, 0.1 mg ml^{-1} glucose oxidase, 0.02 mg ml^{-1} catalase, 1% 2-mercaptoethanol and 3–9% w/w glucose.

Received 20 March; accepted 9 August 2002; doi:10.1038/nature01083.

1. Lohman, T. M. & Bjornson, K. P. Mechanisms of helicase-catalyzed DNA unwinding. *Annu. Rev. Biochem.* **65,** 169–214 (1996).
2. Hall, M. C. & Matson, S. W. Helicase motifs: the engine that powers DNA unwinding. *Mol. Microbiol.* **34,** 867–877 (1999).
3. von Hippel, P. H. & Delagouette, E. A general model for nucleic acid helicases and their "coupling" within macromolecular machines. *Cell* **104,** 177–190 (2001).
4. Patel, S. S. & Picha, K. M. Structure and function of hexameric helicases. *Annu. Rev. Biochem.* **69,** 651–697 (2000).
5. Velankar, S. S., Soultanas, P., Dillingham, M. S., Subramanya, H. S. & Wigley, D. B. Crystal structures of complexes of PcrA DNA helicase with a DNA substrate indicate an inchworm mechanism. *Cell* **97,** 75–84 (1999).
6. Mechanic, L. E., Hall, M. C. & Matson, S. W. Escherichia coli DNA helicase II is active as a monomer. *J. Biol. Chem.* **274,** 12488–12498 (1999).
7. Levin, M. K. & Patel, S. S. The helicase from hepatitis C virus is active as an oligomer. *J. Biol. Chem.* **274,** 31839–31846 (1999).
8. Ali, J. A., Maluf, N. K. & Lohman, T. M. An oligomeric form of E-coli UvrD is required for optimal helicase activity. *J. Mol. Biol.* **293,** 815–834 (1999).
9. Dillingham, M. S., Wigley, D. B. & Webb, M. R. Demonstration of unidirectional single-stranded DNA translocation by PcrA helicase: Measurement of step size and translocation speed. *Biochemistry* **39,** 205–212 (2000).
10. Cheng, W., Hsieh, J., Brendza, K. M. & Lohman, T. M. *E. coli* Rep oligomers are required to initiate DNA unwinding *in vitro*. *J. Mol. Biol.* **310,** 327–350 (2001).
11. Bianco, P. R. *et al.* Processive translocation and DNA unwinding by individual RecBCD enzyme molecules. *Nature* **409,** 374–378 (2001).
12. Dohoney, K. M. & Gelles, J. χ-Sequence recognition and DNA translocation by single RecBCD helicase/nuclease molecules. *Nature* **409,** 370–374 (2001).
13. Weiss, S. Measuring conformational dynamics of biomolecules by single molecule fluorescence spectroscopy. *Nature Struct. Biol.* **7,** 724–729 (2000).
14. Ha, T. *et al.* Probing the interaction between two single molecules—fluorescence resonance energy transfer between a single donor and a single acceptor. *Proc. Natl Acad. Sci. USA* **93,** 6264–6268 (1996).
15. Zhuang, X. W. *et al.* A single-molecule study of RNA catalysis and folding. *Science* **288,** 2048–2051 (2000).
16. Ha, T. Single molecule fluorescence resonance energy transfer. *Methods* **25,** 78–86 (2001).
17. Sofia, S. J., Premnath, V. & Merrill, E. W. Poly(ethylene oxide) grafted to silicon surfaces: grafting density and protein adsorption. *Macromolecules* **31,** 5059–5070 (1998).

18. Chao, K. & Lohman, T. M. DNA-induced dimerization of the *Escherichia coli* Rep helicase. *J. Mol. Biol.* **221,** 1165–1181 (1991).
19. Bjornson, K. P., Amaratunga, M., Moore, K. J. M. & Lohman, T. M. Single-turnover kinetics of helicase-catalyzed DNA unwinding monitored continuously by fluorescence energy transfer. *Biochemistry* **33,** 14306–14316 (1994).
20. Moore, K. J. M. & Lohman, T. M. Kinetic mechanism of adenine nucleotide binding to and hydrolysis by the *Escherichia coli* Rep monomer. 1. Use of fluorescent nucleotide analogues. *Biochemistry* **33,** 14550–14564 (1994).
21. Wong, I. & Lohman, T. M. A two-site mechanism for ATP hydrolysis by the asymmetric Rep dimer P2S as revealed by site-specific inhibition with ADP-AlF4. *Biochemistry* **36,** 3115–3125 (1997).
22. Dillingham, M. S., Wigley, D. B. & Webb, M. R. Direct measurement of single-stranded DNA translocation by PcrA helicase using the fluorescent base analogue 2-aminopurine. *Biochemistry* **41,** 643–651 (2002).
23. Yarranton, G. T. & Gefter, M. L. Enzyme-catalyzed DNA unwinding: studies on *Escherichia coli* rep protein. *Proc. Natl Acad. Sci. USA* **76,** 1658–1662 (1979).
24. Lohman, T. M., Chao, K., Green, J. M., Sage, S. & Runyon, G. T. Large-scale purification and characterization of the *Escherichia coli* rep gene product. *J. Biol. Chem.* **264,** 10139–10147 (1989).

Supplementary Information accompanies the paper on *Nature*'s website (http://www.nature.com/nature).

Acknowledgements We thank C. Chidsey for suggesting the use of a PEG surface, and T. Ho for synthesis and purification of the oligonucleotides. This work was supported by the NSF and AFOSR (S.C.), by the NIH (T.M.L.), and by a Searle scholars award, the NIH, an NSF CAREER award, the Research Corporation, and the UIUC research board (T.H.)

Competing interests statement The authors declare that they have no competing financial interests.

Correspondence and requests for materials should be addressed to T.H. (e-mail: tjha@uiuc.edu).

SATB1 targets chromatin remodelling to regulate genes over long distances

Dag Yasui*, Masaru Miyano*, Shutao Cai*, Patrick Varga-Weisz† & Terumi Kohwi-Shigematsu*

** Life Sciences Division, Lawrence Berkeley National Laboratory, University of California, Berkeley 94720, USA*
† Marie Curie Research Institute, The Chart, Oxted, Surrey RH8 OTL, UK

Eukaryotic chromosomes are organized inside the nucleus in such a way that only a subset of the genome is expressed in any given cell type, but the details of this organization are largely unknown[1–3]. SATB1 ('special AT-rich sequence binding 1'), a protein found predominantly in thymocytes[4], regulates genes by folding chromatin into loop domains, tethering specialized DNA elements to an SATB1 network structure[5]. Ablation of SATB1 by gene targeting results in temporal and spatial misexpression of numerous genes and arrested T-cell development, suggesting that SATB1 is a cell-type specific global gene regulator[6]. Here we show that SATB1 targets chromatin remodelling to the *IL-2Rα* ('*interleukin-2 receptor α*') gene, which is ectopically transcribed in SATB1 null thymocytes. SATB1 recruits the histone deacetylase contained in the NURD chromatin remodelling complex to a SATB1-bound site in the *IL-2Rα* locus, and mediates the specific deacetylation of histones in a large domain within the locus. SATB1 also targets ACF1 and ISWI, subunits of CHRAC and ACF nucleosome mobilizing complexes, to this specific site and regulates nucleosome positioning over seven kilobases. SATB1 defines a class of transcriptional regulators that function as a 'landing platform' for several chromatin remodelling enzymes and hence regulate large chromatin domains.

SATB1 forms a three-dimensional network structure in mouse thymocyte nuclei[5]. It specifically binds to double-stranded DNA with a specialized ATC sequence context that readily becomes base-unpaired in supercoiled DNA[4,7,8]. Such base unpairing regions (BURs) are important elements of matrix attachment regions[7,8]. SATB1 regulates genes located as much as ~50 kilobases (50 kb) away from the attached sites. In SATB1 null thymocytes, which arrest at the $CD4^+CD8^+$ double positive stage, the normal SATB1-bound genomic loci are detached and associated genes are dysregulated[5]. What is the mechanism that connects SATB1 function in nuclear organization to transcription? We tested a hypothesis that the SATB1 network provides assembly sites for chromatin remodelling and modifying factors involved in gene regulation and other nuclear functions[9]. ATP-dependent chromatin remodelling factors use the energy gained by ATP hydrolysis to alter nucleosome array structures[2,10,11]. Histone modifying enzymes are involved in both transcriptional activation (such as histone acetylation) and repression (for example, histone deacetylation)[9].

Using DNA affinity chromatography designed to purify SATB1, we investigated whether chromatin remodelling and modifying factors specifically co-purify with SATB1. We compared elution profiles of extracts prepared from wild-type and SATB1 null thymocytes (+/+ and −/−, respectively). A BUR containing a core unwinding element found in a matrix attachment region 3′ of the immunoglobulin heavy chain (IgH) enhancer was multimerized and used to make a DNA affinity column to purify SATB1. In order to trap non-specific A + T-rich and other DNA binding proteins, thymocyte extracts were first loaded onto a mutated (Mut) BUR column that has lost the unwinding propensity, but retains the A + T-rich feature. The flow-through of this column was applied onto the wild-type (WT) BUR column. As shown in Fig. 1a (middle panel, lanes, SM, Mut, WT), SATB1 flows through the mutant BUR affinity column and is almost completely retained in the wild-type BUR column[12]. SATB1 was eluted from this column by 0.4–0.8 M $[Na^+]$. We asked whether the NURD (nucleosome remodelling and histone deacetylase) complex co-purifies with SATB1. The NURD complex has been implicated in transcriptional repression of several genes[13], and contains ATP-dependent remodelling enzyme Mi-2 (relative molecular mass 240,000; M_r 240K), histone deacetylase 1 (HDAC1; 62K) and 2 (HDAC2; 55K), histone deacetylase associated co-repressor mSin3A (160K) and MTA-2 (70K)[14–16]. In addition, we monitored the presence of nucleosome-dependent ISWI-ATPase (140K), and ACF1 (180K), both subunits of the ACF and CHRAC complexes (reviewed in ref. 17). These complexes are known to mobilize nucleosomes to reorganize nucleosomal arrays over large distances *in vitro*[17]. However, nothing is known about their *in vivo* function, and whether they are targeted to specific sites. In the fractions that contained SATB1, the NURD complex subunits Mi-2, mSin3A, MTA-2, HDAC1 and HDAC2 and CHRAC/ACF complex subunits ACF1 and ISWI, were also detected (Fig. 1a, top panel). These chromatin remodelling factors were retained on the BUR column via SATB1, as none of these proteins were retained when SATB1 deficient extracts were applied (Fig. 1b, top panel). Mi-2, ACF1, mSin3A, ISWI, MTA-2, HDAC1 and HDAC2 proteins were present at roughly the same abundance in a SATB1 deficient thymic extract as the wild-type extract (Fig. 1a, b, SM, Mut and WT lanes). Apparently, chromatin remodelling factors that co-purified with SATB1 represent a subfraction of each of these factors present in thymocytes, as these proteins were also found in the flow-through fraction of the BUR affinity column (Fig. 1a, lane WT). Poly (ADP-ribose) polymerase (PARP), another BUR-binding protein[18] found in both wild-type and SATB1 null thymocyte extracts, was retained in the BUR affinity column (Fig. 1a, b, bottom panels), indicating that the affinity column used for both extracts was active. The data also indicate that unlike SATB1, a BUR-binding protein such as PARP is not sufficient to recruit chromatin remodelling factors to sites of the specialized DNA context. The elution profile of chromatin remodelling factors did not exactly match that of SATB1. One explanation could be that these factors associate with SATB1 less strongly than SATB1 to DNA. Co-elution of chromatin